MODELLING AND EXPERIMENTAL VALIDATION OF THE DYNAMIC STARTUP BEHAVIOR OF EXTERNAL SPUR GEAR MOTOR

Ajinkya Pawar[1], Andrea Vacca[1], Manuel Rigosi[2]

Maha Fluid Power Research Center[1], Purdue University, Lafayette, IN, USA

Casappa S.P.A.[2], Parma, Italy

Abstract.

The sizing of fluid power systems controlling hydraulic motors is often affected by their dynamic start-up behavior. The start-up pressure that must be provided to initiate the rotation of a hydraulic motor is usually significantly higher that the corresponding pressure reached in steady operation, due to internal frictional effects. This important aspect, typically referred to as "startup torque" affects the motor shaft dynamic, as well as the power requested from the hydraulic supply. Despite the importance of this aspect, there are only few modelling techniques, mostly empirical, available to describe the start-up characteristics of hydraulic motors. This paper contributes to this field by presenting a model for the analysis of the dynamic operation of a spur gear motor. The model predicts the start-up pressure and torque, as well as the shaft speed evolution over time. The proposed model builds upon the HYGESim (HYdraulic GEar machine Simulator) developed by the authors' team in the past years. The modeling approach is refined to consider the torque contributions affecting the rotational dynamics of gears. To allow simulating many shaft revolutions in a complete hydraulic system, the torque losses at the lubricating interfaces are interpolated from pre-computed results of a detailed in-house multiphysics simulation model available to the authors. An experimental activity was performed on a commercial motor to validate the model. Experiments allowed to measure the instantaneous flow, pressure, and speed during a start-stop cycle typical of a fan drive system. The experimental and simulation results show very good qualitative and quantitative agreement. The proposed simulation approach can help designers in optimization studies to achieve better designs, owing to its accuracy and reduced simulation time.

Keywords. Gear motors, External Gear Machines, Dynamic modelling, Start-up torque, Hydromechanical Efficiency

1. INTRODUCTION

This paper addresses the topic of modeling the start-up behavior of hydraulic motors, namely the so-called "start-up torque" aspect of this kind of components. To briefly explain the

concept of start-up torque, it is useful to remind the relationship valid at steady state conditions:

$$\Delta p_m = \frac{2\pi T_m}{\eta_{hm} V_d} \tag{1}$$

In this equation T is torque at the motor shaft, and the torque efficiency, η_{hm} represents the steady state torque losses. During transient start-up, the higher friction present at the internal interfaces causes a much larger pressure drop required to induce the shaft rotation. According to Eq. (1), this overpressurization for Δp_m can be perceived as an additional torque present at the shaft, thus leading to a definition of a start-up torque larger than the corresponding steady state value. This start-up torque is a critical parameter for system using hydraulic motors. In fact, the hydraulic control system must be designed considering this more stringent start-up torque condition, rather than a nominal torque given by Eq. (1).

Studies were carried out in the past to understand the start-up process of hydraulic components. Many of these studies were focused upon modelling friction losses at different lubricating interfaces. Harnoy [1] proposed an analytical model to determine start-up torque loss from hydrodynamic journal bearings including stick-slip effects. Bouyer and Fillon [2] along with Henry [3] performed experimental measurements to determine the friction torque from journal and thrust bearings during start-up. In both cases, a high peak in coefficient of friction during start-up was observed. For line contacts a similar experimental study was carried out by Gasenfeit and Soom [4]. Garcia et al [5] presented effects of lubricants on static friction determination at lubricated line contacts. The torque loss during start-up of different types of hydraulic motors was experimentally captured by Michael et al. [6] to study the effects of lubricant chemistry and rheology on starting efficiency. The analytical modelling of the torque losses during start-up of hydraulic motors has been an unexplored area of research. Existing models are either interface specific as in [1] or entirely empirical in nature, as proposed by Merritt [7], Hibi and Ichikawa [8], and not very suitable for design purposes.

Modelling of frictional losses in steady-state operation in external gear pumps was recently presented by Rituraj et al. [9], who considered losses at various lubricating interfaces using analytical formulations, showing accuracy in the prediction of the machine hydromechanical efficiency. However, full film regime in all lubricating interfaces was assumed, which is an unsuitable assumption for start-up.

The present paper aims formulating a model for external spur gear machines (EGMs) suitable for both steady-state operation as well as start-up dynamics. While modelling and experimental analysis of EGMs has been a major area of research for the authors' research group over the past decade, the aspect of dynamic start-up is for the first time introduced. For the purposes of this research, the model is implemented in a Simcenter Amesim environment and is validated against start-up experimental data by comparing the start-up pressure and rotational speed of the motor. The reference machine used for the simulation and experiments is a Casappa Polaris gear motor. The unit is based on a pressure compensated axial balancing design using 4 journal bearings integrated in floating bearing blocks. Important design details of the reference unit are provided in table 1.

Table 1: Reference unit details

Displacement	4.95 cc/rev
Maximum operating pressure	260 bar
Maximum operating speed	4000 rpm
Number of teeth	12
Housing material	Aluminum

The structure of the paper is as follows: Section 2 presents the modelling methodology followed to evaluate the rotational dynamics of the motor. Section 3 includes the description of start-up experimental tests and details of simulation model setup. Results obtained from the simulation model and their comparison with experimental data are presented in Section 4. Additional capabilities of the model in terms of hydromechanical efficiency evaluation are also detailed in Section 4 while Section 5 includes conclusions and possible improvements to the current model that can be done in future

2. MODELING METHODOLOGY

Over the past decade, the authors' research group has developed an external gear machine simulation tool now called Multics-HYGESim. Figure 1 shows the schematic of different submodules of this tool which are used to simulate the operation of an EGM. For completeness, all modules are described here briefly. Further details on the simulation methodology followed by this tool can be found in [10]. The geometrical module extracts important information regarding the geometry of the machine using CAD files of important components such as gears, lateral bushings, and casing. The pressurization of fluid inside tooth space volumes (TSV) of an EGM is modelled by a DC solver using a lumped parameter approach which also considers, tooth tip leakages and cavitation. The Reynolds solver uses a CFD approach to study the details of lubricating interfaces (lateral gap fluid films and journal bearings). The forces calculated by DC and Reynolds solvers are used by Dynamics Solver to determine the instantaneous position of the involved bodies (gears and bushings), also allowing to account for wear-in of the housing. The Deformation Solver accounts for effects of fluid structure interaction by determining the deformation of bodies.

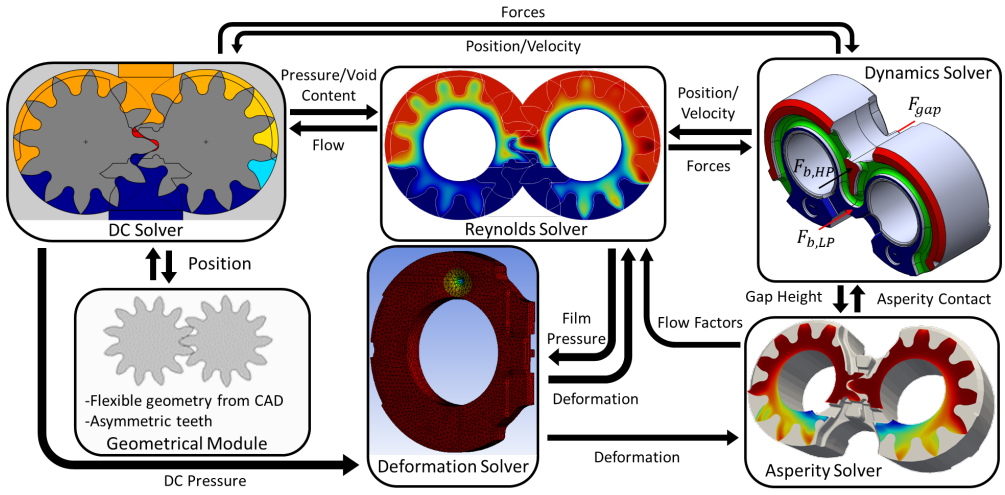

Fig. 2.1- Schematic of Multics-HYGESim

Finally, the asperity solver accounts for mixed lubrication effects at these interfaces. Various aspects of an EGM such as volumetric efficiency, pressure ripple, leakages are simulated and experimentally validated with this simulation tool as described in [10]. However, all these studies were carried out under steady state operating conditions. As Multics-HYGESim adopts a computational approach to simulate the coupled effects of the previously mentioned physical phenomena (CFD approach, mixed lubrication, and fluid structure interaction effects), the computational cost is high, resulting in relatively high simulation times (typically about one day for simulating few revolutions). Thus, simulating the transient behavior of the motor becomes challenging with this approach, as the transient simulation must consider many shaft revolutions. To overcome to this challenge, this paper proposes a reduced model derived from Multics-HYGESim, which considers the aforementioned effects in an analytical way. Additionally, the authors also propose methodology to calculate the start-up torque of the motor as well as to include frictional loss from different sealing interfaces inside the motor. Details of this reduced model (referred to as proposed model henceforth) are presented in the upcoming section focusing on methodology followed to solve the dynamic behavior of an external gear motor.

2.1. External Gear Motor Dynamic Modeling

The inlet side of the motor is connected to a high-pressure line while the outlet side of the motor is connected to a low-pressure line. The pressurized fluid exerts a rotary moment on both gears causing them to rotate in opposite directions. Thus, the fluid is displaced from the high-pressure side to low-pressure side while causing the actuation or generation of rotary motion during this process. Figure 2 depicts the moments acting on gears and their directions under assumed orientation of inlet and outlet, as well as the coordinate system which include moments due to fluid pressure and moments due to friction. Gear 1 is assumed to be driving an external load and thus, is subjected to additional moment due to the resistance and inertia of the load. Considering these moments, Newton's second law is applied to both gears (Eq. 2 and 3), which are assumed as rigid bodies:

$$M_{fp1} + M_{c1} - M_{f1} - M_l = (I_1 + I_l)\alpha_1 \qquad (2.2)$$

$$M_{fp2} - M_{c2} - M_{f2} = I_2\alpha_2 \qquad (2.2)$$

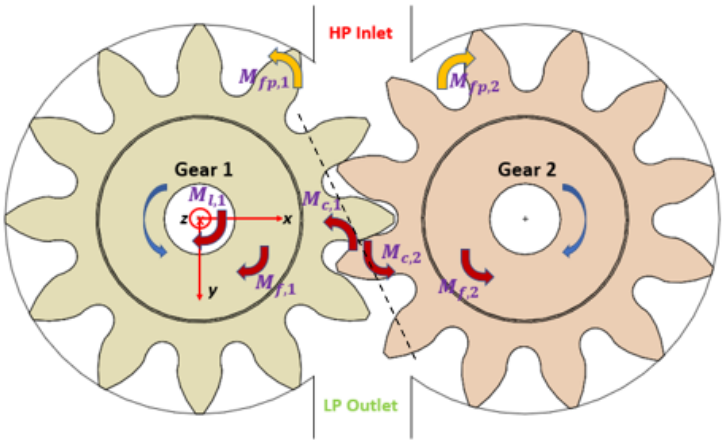

Fig. 2.2 - Loads determining rotational dynamics of gears

2.2. Moment due to fluid pressure

To determine the moment due to fluid pressure acting on the gears, the pressure inside each tooth space volume (TSV) chambers of both gears is first evaluated according to a lumped parameter approach first introduced by Vacca & Guidetti in [11]. This approach is based on the pressure buildup equation (4), and it is also used in the DC Solver of Multics-HYGESim, Fig. 2. The overall pressure distribution in all TSVs is then used to calculate forces and moments acting on both gears. The force loading is then used to describe the radial micromotion of the gears as described in in [11].

$$\frac{dp_i}{dt} = \frac{K_{oil}}{V_i}\left(\sum(Q_{in} - Q_{out}) - \frac{dV_i}{dt}\right) \tag{2.3}$$

It is worth mentioning that gear motors have different gear meshing conditions than gear pumps. In the case of a pump, gear 1 shown in Fig. 2 would be connected to an external prime-mover which rotates the gear such that the fluid is displaced from a low-pressure inlet (LP) to a high-pressure outlet (HP). With the port pressure conditions of Fig. 2, gear 1 would rotate clockwise and gear 2 would be driven by gear 1. Instead, in case of a motor, there is no prime mover. Due to its smaller inertia, gear 2 drives gear 1 which is connected to an external rotary load. This meshing difference must be carefully considered in this work for the accurate evaluation of fluid dynamic characteristics of the motor. To allow using the geometric model previously developed for pumps the current paper considers the inlet and outlet as shown in Fig. 2. Under these conditions, the contact location of both gears remains the same as it would have been if the EGM is operated in pumping mode.

2.3. Moment due to friction

Frictional losses in EGMs generally arise from friction acting at various interfaces which include journal bearings (JB), lateral gap (LG) fluid films, meshing, seals, drain leakage, and tooth tip leakage interfaces.

Differently from the past work [9], where full-film conditions were assumed, this work consider a CFD approach to determine losses at journal bearing and lateral fluid film interfaces by considering effects of mixed lubrication and solid to solid contact friction. Authors here have chosen an approach to account for these effects using independent CFD simulations for the JB and LG interface with the aim of obtaining an analytical implementation to reduce computational time for running motor transient simulations while maintaining accuracy of frictional loss prediction.

2.3.1. Friction at journal bearings

At each journal bearing, shear forces are generated at the shaft and fluid film interface due to presence of viscous as well as contact friction. For analytical implementation, the friction coefficient variation for the reference journal bearing is determined as a function of a suitable non-dimensional parameter by running standalone CFD simulations under operating conditions defined in table 2. This parameter is chosen to be Sommerfield number (Eq. 2.4). For these simulations, the shaft is treated as a rigid body which has free degrees of translational motion in x and y directions and rotating at the prescribed operating speed, while the bushing is treated as a fixed rigid body.

$$S = \frac{\eta N}{P}\left(\frac{r}{c}\right)^2 \tag{2.4}$$

Table 2: Parameters for the standalone journal bearing simulation

Model Parameters	Value [unit]
Shaft Velocity	10-3000 RPM
Load	5500 N
Working fluid	ISO VG 46
Operating Temperature	50^oC
Sommerfield Number Range	0.001-0.2

Simulations are run at a range of Sommerfield number values by varying the operating speed while keeping the applied load on the shaft as constant. The friction force on the shaft is evaluated by integrating the shear stress at the shaft surface. At very low values of Sommerfield number, the bearing operates in mixed lubrication regime. In this case, contribution of surface roughness to fluid film behavior cannot be ignored. To model this, a stochastic approach presented by Patir and Cheng [12] is used. In this regime, the fluid film cannot support the entire load and partial load support is offered by asperity contact. Thus, the friction force for this regime consists of the force due to shear stress in mixed lubrication (Eq. 6) and the friction force due to asperity contact (Eq. 7).

$$\tau_w = \varphi_{fp}\frac{h}{2}\frac{\partial p}{\partial x} + (\varphi_f + \varphi_{fs})\frac{\eta(U_2 - U_1)}{h} \tag{2.5}$$

$$F_{f,asp} = \mu_{asp}\int p_{asp} dA_{asp} \tag{2.6}$$

Based on simulation results, data for coefficient of friction variation with respect to Sommerfield number is acquired. This data is used to obtain a curve fit to calculate the coefficient of friction at the journal bearing analytically, Eq. (8). The torque loss at journal bearing is then obtained using Eq. (9).

$$\mu_{JB} = 0.04486 * e^{-\left(\frac{S}{0.002681}\right)} + 0.01897 * tanh\left(\frac{S}{1.085}\right) + 0.0006507 \tag{2.7}$$

$$M_{JB} = \mu_{JB} r_s F_s \tag{2.8}$$

2.3.2. Friction at lateral fluid film interface

The lateral fluid films in pressure compensated EGMs provide axial load support which is beneficial for axial balancing of such units. Past work by the authors' research group, such as [9], presented a fast analytical approach to calculate the torque loss at this lubricating interface. In particular, the friction moment generated due to shear stress was calculated also considering possible tilting of the floating bushings with respect to gears. Even though this approach is computationally suitable as it uses closed form solutions, it does not consider effects of gear and lateral bushing deformation, mixed lubrication and asperity contact friction, which instead heavily affect start up conditions. To capture these

effects, this work has considered complete simulations of the reference machine with the Multics–HYGESim introduced earlier.

Figure 7 shows the difference in predicted torque loss at lateral films obtained using the proposed approach and the analytical approach previously used in [9]. Torque loss values are non dimensionalized for confidentiality reasons. These plots clearly indicate how the analytical model described in [9] underpredicts friction losses at lateral films for all operating conditions. To capture the extra torque loss a term ΔM_{LG} is defined as in Eq. 10 and considered in the proposed model to avoid running computationally expensive CFD simulations.

$$\Delta M_{LG} = M_{CFD,lat} - M_{analytical,lat} \qquad (2.9)$$

To describe ΔM_{LG} in a model that does not evaluate the hydrodynamic effects in the lateral films as in Multics-Amesim, the gear side film pressure distribution is approximated using TSV chamber pressures. As a result, an unbalanced force in the axial direction of the bushing (F_z) and an unbalanced tilting moment about horizontal axis of the bushing (M_x) is observed on the lateral bushing. The approach taken is to model the extra torque loss ΔM_{LG} as a function of F_z and M_x. A lookup-table which outputs the value of ΔM_{LG} corresponding to values of F_z and M_x is obtained by interpolating the available data (Fig. 3).

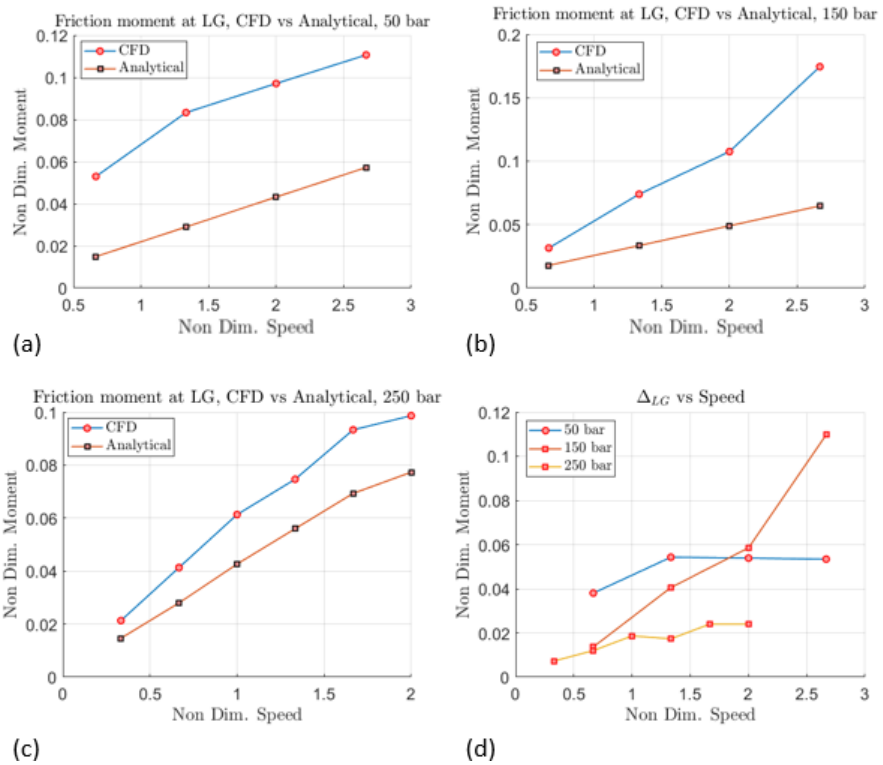

Fig. 2.3: Comparison of friction loss at lateral interfaces a) 50 bar b) 150 bar c) 250 bar inlet pressure d) Map of difference between torque loss predicted

2.3.3. *Friction at Meshing Interface*

During meshing, a rolling and sliding contact occurs between gears teeth, which leads to friction at this interface. In spur EGMs, this contact is non-conformal in nature. Due to high contact loads and small contact area, fluid pressure in this region is in the order of gigapascals causing local elastic deformation of the bodies and modifying the gap height distribution. Thus, meshing zone contact shows presences of Elasto-Hydrodynamic Lubrication (EHL). This work uses the same approach as in reference paper [9], which consists on using the Jacobson and Hamrock model [13] to determine coefficient of friction in EHL conditions.

.

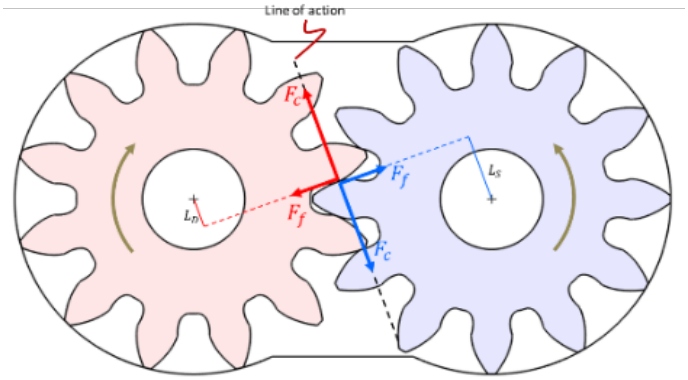

Fig 2.4: Friction moment at gear meshing interface

In particular, the friction force at meshing interface is determined by multiplying a coefficient of friction, Eq. (11) by the contact force. The moment due to this force is determined by multiplying it with a moment arm as shown in Fig. 4. The meshing friction moment on gears, can either support or oppose the motion. But the net effect always results in a torque loss.

$$\mu_1 = 0.6710^{-6}(U^*)^{0.81}U^{0.26}(WG^2)^{3.32} \text{ if } \mu_1 \leq 0.8\gamma$$
$$\mu_1 = 0.80\gamma + 0.021\tanh\left(\frac{\mu_1}{\gamma} - 0.8\right) \quad \text{if } \mu_1 > 0.8\gamma \tag{2.10}$$

2.3.4. *Friction at tooth tip interface*

The geometry of EGMs allows tooth tip leakages to be treated as laminar flow between parallel plates. The net friction force at these interfaces is calculated by integrating wall shear stress, which includes the contribution of both Couette and Poiseuille terms of laminar flow as indicated in reference [9]. Eq. (12) is used to determine the shear stress and in turn, frictional loss at this interface can be calculated using Eq. (13).

$$\tau_{w,i} = \frac{\omega r_g \eta}{h} + \frac{h(p_{i+1} - p_i)}{2L} \tag{2.11}$$

$$M_{tip} = \sum_i F_i r_g = Lbr_g \sum_i \tau_{w,i} \qquad (2.12)$$

2.3.5. Friction at seals in EGMs

To prevent leakages from different pressurized areas, the reference machine uses rubber seals are used as shown in Fig. 5. A shaft seals prevents leakage from the drive gear shaft to the outside of the unit. Seals on the balance side of the bearing blocks seal the environments between HP and LP balance areas. While assembly the EGMs, seals are subjected to pre-load to ensure proper operation which result in friction and torque loss at these interfaces.

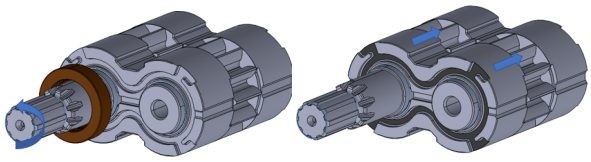

Fig 2.5: Major Seals inside the reference EGM a) Shaft Seal b) Bearing Block Seal

The shaft seal compresses against the drive shaft and the casing, which results in friction generation at the interface causing torque loss to occur. To estimate the value of this loss, a 2006 study by Nikas and Sayles [14] is referred. According to their study, the hydrodynamic friction force on the rotor and stator separated by a seal is dependent on penetration depth and temperature. The value of hydrodynamic friction force at shaft seal interface is determined based on Fig 6. This value is assumed to be constant. This assumption is valid because the load support from forces acting in radial direction on gears is provided by the journal bearings, which leads negligible change in radial forces at seal interface. The penetration depth at the seal does not change and can be assumed to be equal to the value established during the initial assembly. The torque loss from shaft seal is determined by multiplying the friction force value taken from [14] by shaft radius.

The bearing block seals contribute the torque loss of EGMs due to an initial pre-load. As shown in Fig. 5 b), the lateral bushings are pushed towards the gear side, due to forces from the balance side. The pre-load of the seal results in an additional force which causes a reduction in the lateral gap height. Thus, the pre-load at bearing block seal influences lateral fluid film behavior and its torque loss. The effect of this additional force is accounted for by including an additional force in axial direction from balance side which changes F_z and M_x on lateral bushings, thus changing the value of ΔM_{LG} of Eq. (10) obtained from interpolation. This additional pre-load is dependent on manufacturing tolerances and is assumed to be constant for the given reference machine.

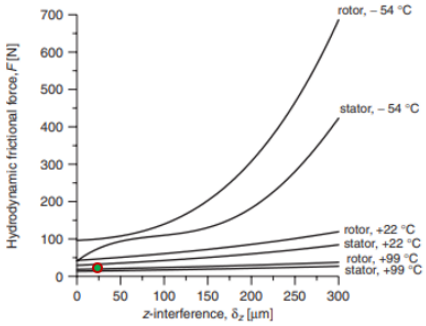

Fig 2.6: Friction force at flexible seals under motion as a function of temperature [14]

2.4. Start-up torque loss modeling

During start up, lubricating interfaces such as journal bearings and lateral films are in boundary lubrication regime leading to high torque loss. Similarly, friction meshing interface during start-up is also seen to be higher as the load is supported mainly by asperities due to lack hydrodynamic support. As the motors speed starts increasing, the operation of these lubricating interfaces transitions from boundary lubrication regime to mixed lubrication and subsequently full film region. This behavior can be modelled using a Stribeck curve.

Analytical modelling of Stribeck curve to predict the frictional force as a function of velocity has been presented in [15]. Thiagarajan et al. [16] used this model to predict the friction force (Eq. 14) at the lateral bushing-casing interface. The same friction model ([16]) is modified to calculate the start-up torque loss in an EGM (Eq. 15). To apply this equation for start-up torque loss, the moment is expressed as a function of angular speed of the motor. Term F_c in Eq. 14 represents the coulomb friction at the boundary lubrication interface.

$$F_f = \sqrt{2e}(F_{brk} - F_c) * \exp\left[-\left(\frac{v}{v_{st}}\right)^2\right] + F_c \tanh\left(\frac{v}{v_c}\right) + fv \tag{2.13}$$

$$M_s = \sqrt{2e}(M_{brk} - M_c) * \exp\left[-\left(\frac{\dot{\theta_m}}{\dot{\theta}_{st}}\right)^2\right] + M_c \tanh\left(\frac{\dot{\theta}}{\dot{\theta}_c}\right) + f\dot{\theta_m} \tag{2.14}$$

It is to be noted that Eq. (15) models the start-up torque to required overcome frictional resistance from all lubricating interfaces of the motor. From Eq. (14), as the velocity increases beyond v_{st}, the friction value is given by summation of coulomb friction component F_c and viscous friction component F_v. Similarly in Eq. (15), the term M_c can be equated to friction moment from shaft seal interface as it is independent of operating speed. Thus, Eq. (15) models the start-up torque loss when motor speed is lower than $\dot{\theta}_{st}$ and torque loss from shaft seal at higher speeds. Values of parameters $\dot{\theta}_{st}$, $\dot{\theta}_c$ and f in Eq. (15) are assumed based on equivalent values in [16]. The value of braking moment M_{brk}, which is the maximum frictional moment that must be overcome for the motor to start rotating, is the only key model parameter that requires tuning based on experimental data.

2.5. Moment due to load

While in operation, hydraulic motors are subjected to external loads which affect their dynamic behavior. Therefore, a dynamic model for these loads is required for modeling the dynamic behavior of the EGM. As it will be discussed in the next section, the reference tests are performed with the motor connected to a fan. The moment from such loads can be modeled as a viscous loss due to air resistance and inertia of the body. In the current model, the inertia of the load is added to the inertia of the gear 1 shaft as shown by Eq. (2). The air resistance is calculated using an empirical linear plus cubic relationship which is generally valid for loads such as a fan.

$$M_{fan} = k_{f1}\omega + k_{f2}\omega^3 \qquad (2.15)$$

The final structure of the reduced model as described in this section is shown in the Fig. 7.

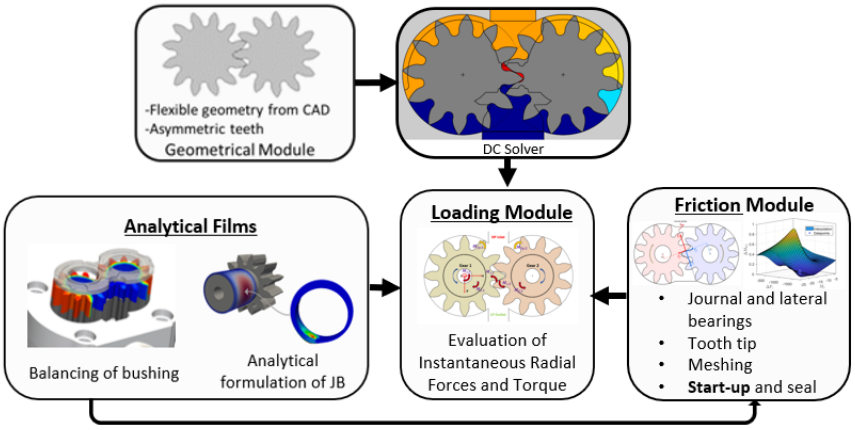

Fig 2.7: Schematic of reduced HYGESim model for transient simulations

3. EXPERIMENTAL SETUP AND SIMULATION MODEL

This section illustrates the experimental setup used to validate the model based on test performed on the reference EGM of table 1. The test schematic is provided in Fig. 8, and the main features of the sensors are provided in table 3. The test set up reproduces a typical hydraulic circuit for fan drive. The motor is supplied with a periodic flow by acting on the shaft speed of the speed pump, which varies from null to a given value. Consequently, the motor starts from rest, reaches a maximum speed and then comes again to rest.

Table 3: Summary of sensor specifications

Sensor	Model	Specifications	Accuracy
Pressure Transducer (P_1)	Parker SCPT-400	0-400 bar	±0.5% Full scale
Pressure Transducer (P_2)	Parker SCPT-400	0-400 bar	±0.5% Full scale
Flowmeter	Parker SCVF-060	0-60 L/min	±0.5% Full scale
Velocity Transducer (pump)	CCT transducers TR10	0-9000 RPM	±0.5% Full scale

Torque Transducer (pump)	CCT transducers TR10	0-250 Nm	±0.1% Full scale
Velocity transducer (motor)	Parker SCRPM-220	0-10000 RPM	±0.5% Full scale

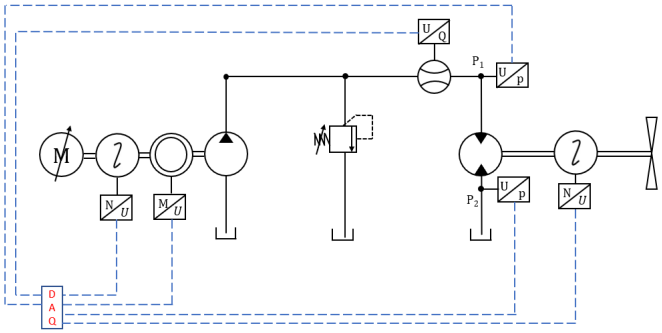

Fig. 3.1: Schematic of experimental setup

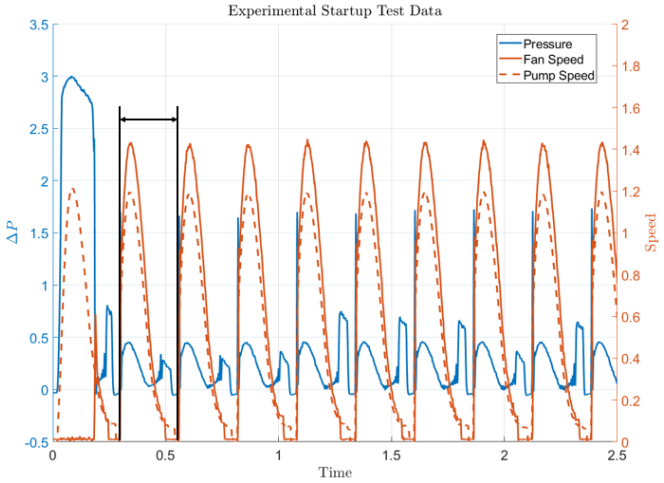

Fig. 3.2: Schematic of non dimensionalized experimental data

The measured pressure differential across the motor and the fan speed is used to validate the simulation model. The flow provided by the supply pump is estimated by the measured pump shaft speed and its volumetric efficiency map. The Hydraulic line connection between the pump and the motor is modelled by considering equivalent thickness and bulk modulus of the rubber hoses using pressure build-up equation (4). The load dynamic of the fun is governed by Eq. (16). As the experimental data is periodic, simulations are carried out for only one period of 20 seconds, marked in Fig. 9, which involves starting up and stopping of the motor.

4. RESULTS

This section provides comparison between experimental and simulated data for start-up pressure, motor pressure drop, and speed evolution over time. All results are non-

dimensionalized with respect to an undisclosed value of equivalent units for confidentiality. Table 4 shows the parameters which are used to obtain results presented in this section.

Figure 10 shows the comparison of motor fan transient speed obtained from simulation and experiments. Results for motor pressure drop comparison are shown in Figure 11. The simulation model captures the transience of fan speed and pressure accurately. The maximum pressure reached during this operation is defined as motor's startup pressure. The simulation predicts the start-up pressure to be almost 400% of maximum operational pressure during experimental cycle and agrees well with experimentally observed value.

Table 4: Motor simulation model calibrated parameters

Model Parameters	Value [unit]
Linear viscous loss coefficient (k_{f1})	0.0002 Nm/rpm
Cubic viscous loss coefficient (k_{f2})	4e-7 Nm/rpm
Braking friction moment (M_{brk})	1 Nm
Load moment of inertia (I_l)	0.0035 kgm^2
Seal friction loss (M_{seal})	0.15 Nm
Hydraulic line length (L)	2.5 m
Temperature	88^oC

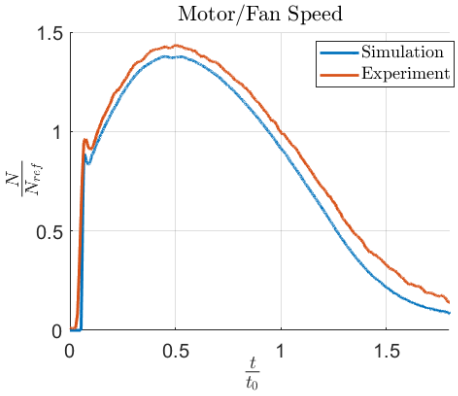

Fig. 4.1: Fan speed evolution with time – comparison between simulations and experiments

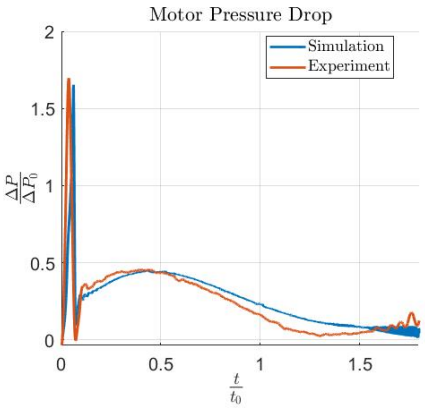

Fig. 4.2: Pressure evolution with time – comparison between simulations and experiments

An offset is seen in the predicted fan speed with respect to the experimental trend during transience. A possible reason can be given by inaccuracies in volumetric efficiency mapping which is used to estimate the inlet flow. During the start-up regime, the speed rise is seen to be more gradual in experimental case while the simulation shows a stiffer behavior. A similar effect is also seen in pressure plots leading to stiffer rise in start-up pressure. Regardless of small inaccuracies, the simulation model matches experimental behavior in terms of trends and magnitude in both start-up and transient regions. Thus, dynamic behavior of an external gear motor can be modelled using the simulation approach described in this paper.

4.1. Additional Model Capabilities – Prediction of hydromechanical efficiency

The presented model that predicts the moment loss due to friction at various interfaces can also be used to estimate the steady state hydromechanical efficiency of the reference unit. Example results for this parameter are compared with experimental data and are presented in a non-dimensionalized form in figure 12.

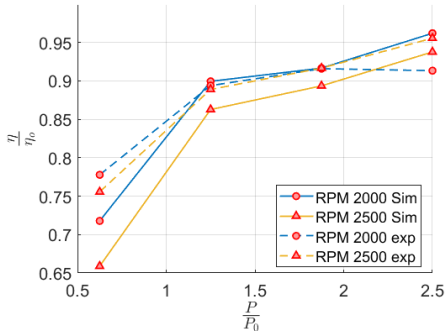

Figure 12: Hydromechanical Efficiency – comparison between simulations and experiments

The model captures the overall hydromechanical efficiency values and trends as seen in experimental data. The inaccuracies observed can be due to inaccurate estimation of seal loss with respect to different operating conditions. Another factor is the journal bearing model which does not account for deformation of shaft and bearing blocks, which can lead to inaccurate torque predictions at that interface.

5. CONCLUSIONS

This paper presents the modelling of the start-up transient features of external gear motors through a fast-modelling approach suitable for the analysis of the typical transient durations of such units. The modelling approach evaluates the net moment on both gear shafts arising from the pressurization of the tooth space volumes, as well as the frictional losses. The friction moments at the lubricating interfaces such as journal bearings and lateral films were determined using a CFD approach including effects of mixed lubrication and integrated in the reduced order model thought an analytical formulation to reduce computational time. Start-up torque loss was determined using a Stribeck curve-based approach, whose characteristics can be easily set by the user. Experiments were performed on a reference unit replicating a typical fan drive system, The predicted start-up pressure and motor speed results showed very good match with respect to experimental start-up test data.

As an additional capability, model shows the capability for predicting hydromechanical efficiency trends and levels at different operating conditions. The model has a potential for further refinements such as modelling the dynamics during stopping of motor. Effects of the solid body deformation of the shaft and the bearing block could be included in the torque loss determination at the journal bearing interface to further increase the model accuracy. Nevertheless, the fast computation time and high accuracy makes the proposed model suitable for performing system design analyses, and also component design optimization studies.

6. NOMENCLATURE

$M_{fp1,2}$	Moment due to fluid pressure on gears 1,2
$M_{f1,2}$	Moment due to friction on gears 1,2
$M_{c1,2}$	Moment due to contact of gear teeth on gears 1,2
M_l	Moment due to load
$I_{1,2}$	Moment of inertia of gears 1,2
I_l	Moment of inertia of load
$\alpha_{1,2}$	Angular acceleration of gears 1,2
p	Fluid pressure
K_{oil}	Bulk Modulus of working fluid
V_i	Volume of i^{th} TSV chamber
$Q_{in,out}$	Flow entering, exiting TSV chamber
τ_w	Wall shear stress at lubricating interfaces
r_s	Shaft radius
η	Lubricant viscosity
$\varphi_{f,fp,fs}$	Flow factors in mixed lubrication model
μ	Coefficient of friction
F_f	Friction force
$U_{1,2}$	Surface velocities at top and bottom surface of lubricating interfaces
S	Sommerfield number
M_{tip}	Friction moment at tooth tip interface
h	Gap height
L,b	Depth, width of gear tooth
r_g	Gear outer radius
M_s	Torque loss at start-up
M_{brk}	Braking friction moment at start-up
M_c	Coulomb friction moment at start-up
f	Viscous friction loss coefficient at seals
$\dot{\theta}_m$	Motor angular speed
$\dot{\theta}_{st}$	Stribeck characteristic speed
$\dot{\theta}_c$	Coulomb characteristic speed
M_{fan}	Viscous torque loss for a fan drive

7. REFERENCES

[1] A. Harnoy, "Model-Based Investigation of Friction During Start-Up of Hydrodynamic Journal Bearings", J. Tribol. 1995, 117(4), pp. 667-673.

[2] Bouyer J, Fillon M. Experimental measurement of the friction torque on hydrodynamic plain journal bearings during start-up. Tribol Int 2011;44:772–81

[3] Y. Henry, J. Bouyer, M. Fillon, Experimental analysis of the hydrodynamic effect during start-up of fixed geometry thrust bearings. Tribology International 2018;120:299-308

[4] E. H. Gassenfeit, A. Soom, Friction Coefficients Measured at Lubricated Planar Contacts During Start Up. Journal of Tribology 1988; 110:533-538

[5] J. Garcia, J. Lumkes, B. Hecahman, A. Martini, Viscosity Dependence of Static Friction in Lubricated Metallic Line Contacts, Tribology Transactions 2011; 54: 333-340

[6] P. Michael, J. Garcia, S. Bair, M. Devlin and A. Martini, Lubricant Chemistry and Rheology Effects on Hydraulic Motor Starting Efficiency, Tribology Transactions 2012; 55:549-557

[7] H. E. Merritt, Hydraulic Control Systems, Wiley Publisher, New York, 1967

[8] A. Hibi, T. Ichikawa, Mathematical Model of the Torque Characteristics for Hydraulic Motors, Bulletin of JSME, 1977; 20-143:616-621

[9] R.Rituraj, A. Vacca, M. Rigosi, Modelling and validation of hydro-mechanical losses in pressure compensated external gear machines, Mechanism and Machine Theory 161 (2021) 104310

[10] T. Ransegnola, F. Zappaterra, A. Vacca, A strongly coupled simulation model for external gear machines considering fluid-structure induced cavitation and mixed lubrication, Applied Mathematical Modelling, Volume 104, 2022, Pages 721-749.

[11] A. Vacca, M. Guidetti, Modelling and Experimental Validation of external spur gear machines for fluid power applications, Simul. Model. Pract. Theory. 19 (2011), 2007-2031

[12] N. Patir, and H. S. Cheng, "An Average Flow Model for Determining Effects of Three-Dimensional Roughness on Partial Hydrodynamic Lubrication." ASME. *J. of Lubrication Tech*. January 1978; 100(1): 12–17. https://doi.org/10.1115/1.3453103

[13] B.O. Jacobson, B.J. Hamrock, Non-Newtonian fluid model incorporated into elastohydrodynamio lubrication of rectangular contacts, J. Tribol. 106 (1984) 275–281, doi:10.1115/1.3260901

[14] G. Nikas, R. Sayles, Study of leakage and friction of flexible seals for steady motion via a numerical approximation method, Tribology International 39 (2006) 921–936

[15] B. Armstrong and C. de Wit. Friction Modeling and Compensation. CRC Press, 1995 edition

[16] D. Thiagarajan, A. Vacca, S. Watkins, On the lubrication performance of external gear pumps for aerospace fuel delivery applications, Mechanical Systems and Signal Processing, Volume129, 2019, Pages 659-676.

Biographies

Ajinkya Pawar completed his bachelor's degree in mechanical engineering and master's degree in Robotics from Indian Institute of Technology Madras, in 2020. He started pursuing a doctorate degree in mechanical engineering at Purdue University under the guidance of Prof. Andrea Vacca. His interests are in numerical modeling of external gear machines considering deformation and thermal effects.

Andrea Vacca is the Maha Fluid Power Faculty Chair and a Professor at Purdue University. He currently leads the Maha Fluid Power Research Center which was established in 2004 by the late Prof. Monika Ivantysynova. Dr. Vacca completed his studies in Italy (Ph.D. from the University of Florence in 2005), and he joined Purdue University in 2010 after being an Assistant Professor at the University of Parma (Italy). Fluid power technology has been Dr. Vacca's major research interest since 2002. Dr. Vacca authored the textbook "Hydraulic Fluid Power" by Wiley and more than 150 technical papers, most of them published in international journals or referred conferences. He is chair of Fluid Power Systems and Technology Division (FPST) of the American Society of Mechanical Engineers (ASME), and a former chair of the Fluid Power Division of the Society of Automotive Engineers (SAE). Dr. Vacca is also one of the Directors of the Global Fluid Power Society (GFPS).

Manuel Rigosi completed his MSc degree in Mechanical Engineering from the University of Parma, in 2011. After an internship, he joined Casappa R&D Department in the role of Simulation Engineer, focused in replicating the physical phenomena within hydraulic gear and piston pumps through the usage of customized lumped parameter models and 3D simulations. In 2018 he took the responsibility for the development of new products with a team of engineers and designers. In recent years he has contributed to innovation by signing 4 patents regarding solutions already applied to the latest products Casappa is offering on the market today.